EFFECTS OF STONE COLUMN INSTALLATION

Richard Kelly[1,2,3] and Chenhui Lee[4]
[1]*Chief Technical Principal Geotechnical, SMEC Australia*
[2]*Honorary Professorial Fellow, University of Wollongong*
[3]*Conjoint Professor of Practice, University of Newcastle*
[4]*Senior Associate, SMEC Australia*

ABSTRACT

Lateral soil displacements caused by stone column installation can be estimated using analytical methods. These analytical methods have been used to assess lateral movements measured during installation of single stone columns and generated by installation of a group of columns. The analytical methods were able to closely match lateral displacements during installation of single stone columns but were less accurate for group installation. Excess pore pressures generated by installation of the group of stone columns was also measured and the peaks could be reasonably approximated using analytical methods. Installation of the group of columns was also simulated using finite element methods. A numerical model based on in-situ and laboratory test data produced similar results to the analytical methods. Refinement of the parameters to better fit the measured data required a four order of magnitude increase in the permeability. It is speculated that such an increase in permeability is created by fracturing of the soft clay during installation of the stone columns. A finite element limit analysis was performed to assess whether the soft clay would be squeezed into the columns. The results of the assessment suggest that it is unlikely that the soft clay would penetrate further than about 2 rows of stone particles.

1 INTRODUCTION

Installation of vibro-replacement stone columns commences with the vibrator penetrating to the design depth into the soft clay using its self-weight and vibration. The vibrator has a diameter of approximately 300mm. Stone is fed into the top of the vibrator via a hopper and the stone falls through the inside of the vibrator and comes out at the base of the vibrator as the vibrator is lifted. The vibrator is then lowered into the stone to densify the stone and laterally displace the stone. The process is repeated until the required diameter has been achieved and until the stone column is constructed to the ground surface.

Stone columns can be constructed to various diameters up to about 1.4m. Construction of the column creates radial expansion from about 0.3m up to 1.4m with associated lateral soil movements within the soil mass. The lateral soil movements have the potential to damage any existing infrastructure in the area adjacent to the newly installed stone columns. Predicting potential lateral soil deformations is therefore a key issue for design.

Measurements of lateral deformation at a point after installation of 4 single stone columns installed at different distances from an inclinometer during construction of the Ballina Bypass has been reported by Kelly et al (2011). Stone columns with a diameter of 1.05m were installed at distances of 2.5m, 5.0m, 7.5m and 10.0m of an inclinometer. The maximum lateral movement recorded at the inclinometer after each stone column was installed was plotted with radius and compared with analytical solutions reported by Carter (1979) and Yu (2000).

The analytical expressions are provided as Equations 1 and 2 below.

$$\rho_r = \sqrt{r^2 + \beta r_0^2} - r \qquad \text{(Carter et al, 1979)}$$

$$\rho_r = \frac{s_u}{2G}\left(1 + \ln\frac{G}{s_u}\right)\left(\frac{r_0}{r}\right)^2 r \qquad \text{(Yu, 2000)}$$

In Equations 1 and 2, ρ_r is radial displacement, r is radius within the soil mass, r_0 is initial cavity radius, s_u is the undrained shear strength of the soil, G is the shear modulus and β is a ratio of net to gross pile area. To fit the measured data a β value of 0.59 and a G/s_u equal to 4.1 was required.

The results of the study are shown in Figure 1.

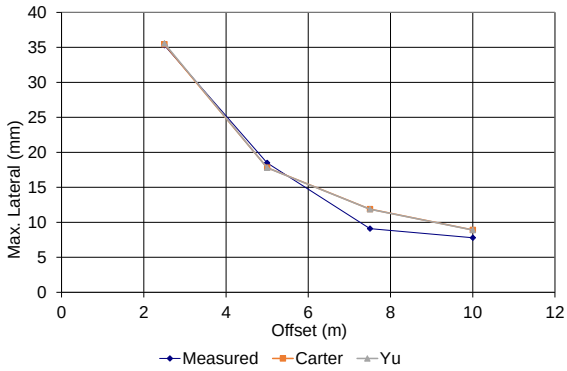

Figure 1: Comparison of measured and interpreted maximum lateral deformations

In 2012, Keller Ground Engineering installed 50 stone columns at the site which would become Australia's National Soft Soil Field Testing Facility near Ballina. Prior to their installation, an inclinometer and three vibrating wire piezometers were installed in order to measure lateral displacements and excess pore pressures. The data is reported in this paper and is compared to predictions for single column installation using Equations 1 and 2. Two and three dimensional finite element analyses (FEA) have also been performed in an attempt to gain further insight into soil displacements and excess pore pressure during installation of stone columns. Finite element limit analyses (FELA) have also been performed to assess the likelihood that the soil flows into the stone column during installation.

2 GROUND CONDITIONS

Ground conditions and material parameters at the Ballina field testing facility have been extensively reported by Pineda et al (2016) and Kelly et al (2016). Typical data with depth obtained by Pineda et al (2016) is shown in Figure 2. The location where the stone columns were installed is shown on Figure 3. A 1m thick fill platform overlies the soft ground at this location. The depth of soft soil is approximately 13m below original ground level.

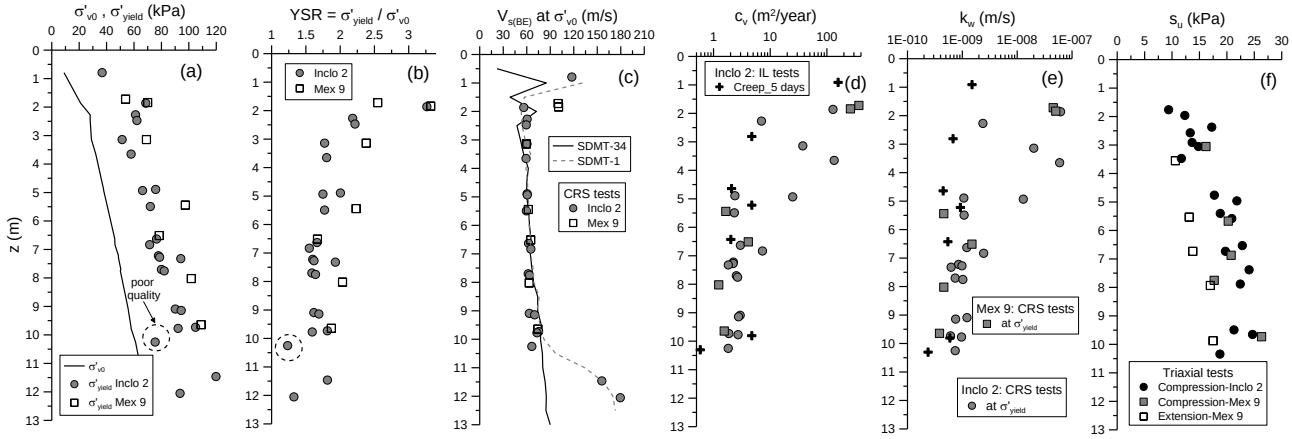

Figure 2 Soil material data

3 GROUP OF STONE COLUMNS

The set out of the stone columns and the instrumentation is shown in Figure 4. The stone columns were installed in three groups with nominally 0.8m, 1.0m and 1.2m diameters. Installed diameters were inferred from volumetric stone consumption and were 0.89m, 1.05m and 1.36m respectively. The stone columns were spaced at 2m centre to centre spacings in both the directions. Basalt stone was used graded between 20mm and 40mm. The peak friction angle of the stone obtained from 300mm diameter shear box tests ranged from 50 degrees to 70 degrees when densely compacted and the constant volume friction angle ranged between 40 degrees and 50 degrees.

The order of stone column installation was 46, 41, 36, 47, 48, 42, 43, 37, 38, 49, 50, 44, 45, 39, 40, 31, 32, 21, 22, 26, 16, 34, 35, 30, 33, 29, 28, 23, 24, 25, 27, 17, 18, 19, 20, 11, 12, 13, 14, 15, 6, 1, 7, 2, 8, 3, 9, 10, 4 and 5.

The stone columns were installed between 3 August 2012 and 17 August 2012. The inclinometer readings are shown in Figure 5 during installation of the columns. The inclinometer was damaged and unreadable after installation of stone column 1 and prior to installation of stone column 2.

Data from vibrating wire piezometers VWP1 and VWP2 are shown in Figure 6. These two piezometers were installed within conventional sand pockets sealed with bentonite pellets. Vibrating wire piezometer VWP3 was sealed with grout and it was found that it responded differently to VWP1 and therefore the data is not reported here.

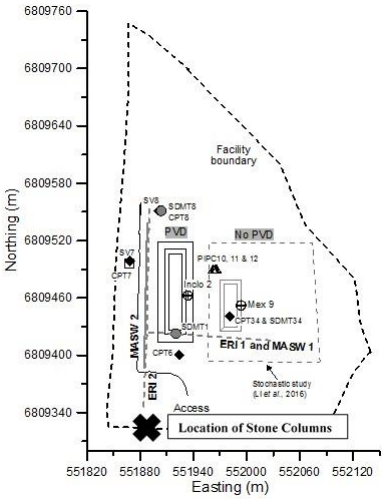

Figure 3: Location of stone column installation

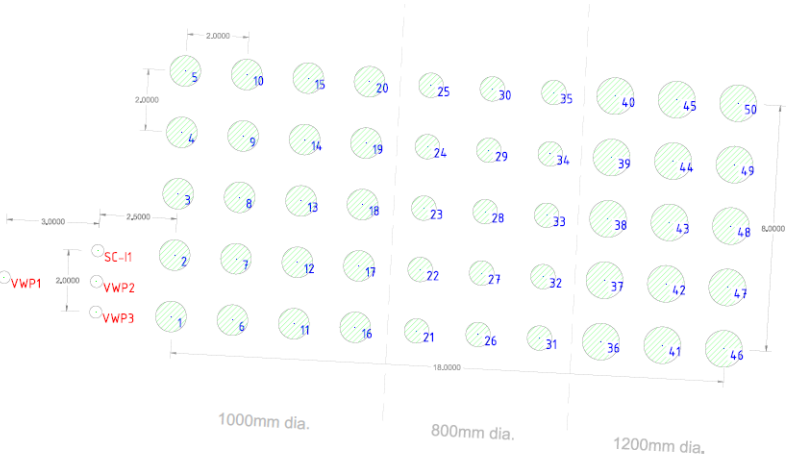

Figure 4: Set out of stone columns

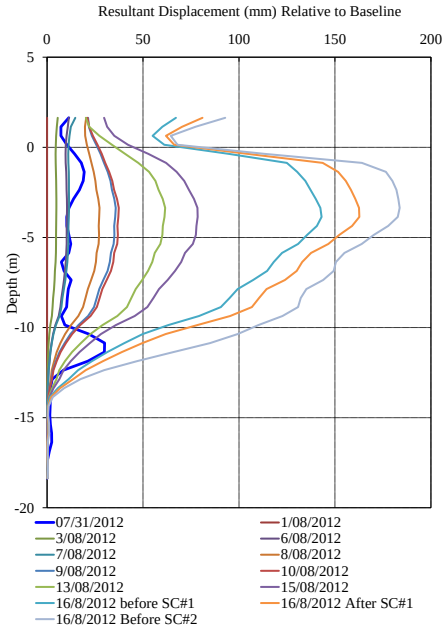

Figure 5: Inclinometer data

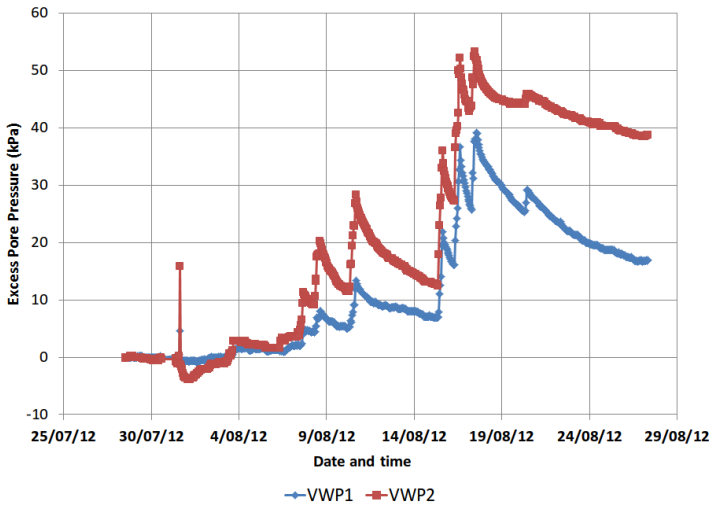

Figure 6: Piezometer data

4 COMPARISON WITH ANALYTICAL METHODS

The maximum lateral displacement recorded over time is compared with Equations 1 and 2 in Figure 7. The data shows that Equations 1 and 2 substantially over-predict the recorded lateral deformations. A better fit to the data using Equation 1 can be obtained using $\beta = 0.15$ to 14 August 2016 and $\beta = 0.48$ thereafter. These β factors indicate that soil displacements caused by expansions of the stone column volume is not being fully transferred to the location of the inclinometer and the factors suggest that only 15% to 50% of the volumetric expansion is being transferred.

Excess pore pressures can be calculated using cavity expansion theory using Equation 3 (Yu, 2000), ignoring the component of excess pore pressure outside the plastic zone. In Equation 3, U is the excess pore pressure, a is the cavity

radius taken as stone column radius, a_0 is the initial cavity radius taken as 0.15m and r is the radius from the centre of each stone column to the vibrating wire piezometer. The rigidity index G_0/s_u was taken to be 350 based on small strain stiffness and undrained shear strength data reported by Pineda et al (2016). Excess pore pressures calculated using Equation 3 are compared with measurements in Figure 8 and can be seen to underpredict measured excess pore pressure.

$$U = s_u \ln\left(\frac{\left(\frac{a}{r}\right)^2 - \left(\frac{a_0}{r}\right)^2}{1 - e^{-\frac{s_u}{G_0}}}\right) \quad (3)$$

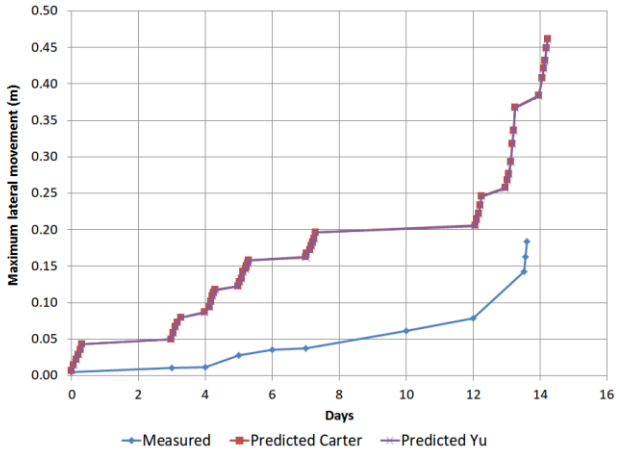

Figure 6: Lateral movements from cavity expansion

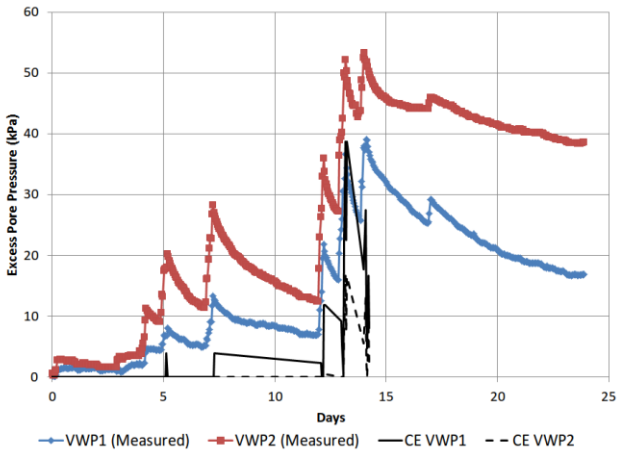

Figure 7: Excess pore pressures from cavity expansion

5 FINITE ELEMENT ANALYSIS

5.2 PLAXIS 2D MODEL

The 2D model aimed to simulate the effects of installation at a depth equivalent to the depth where maximum lateral deformation was measured. A 100m by 100m mesh was generated with lateral fixity at the left hand edge and vertical fixity applied at the base of the mesh. Stresses were used at the upper and right hand side boundary conditions. A stress of 30kPa was applied which is designed to simulate the in-situ horizontal pressure at the relevant depth. The stone columns were modelled as hexagons having an area equivalent to a circle of 300mm diameter. The 15 noded isoparametric elements were used.

The HS Small model was used to simulate the soil. Key material parameters used in the analyses are summarised in Table 1. Definitions of the parameters can be found in the Plaxis manual. A simulation of an undrained triaxial test using these parameters with a confining pressure of 30kPa is shown in Figure 9. The parameters in Table 1 were selected in order to generate a broadly similar triaxial stress-strain response to data shown in Pineda et al (2016) for soils tested at similar depth. However, that has resulted in stiffness values in Table 1 being greater than reported by Pineda et al (2016). Analyses were performed using two soil models, the difference being the permeability which differs by about three orders of magnitude. A permeability of 8.64E-5 m/day is similar to that recorded by Pineda et al (2016).

Table 1: Material Properties used in Plaxis 2D analyses

Material	γ (kN/m^3)	Void Ratio (e_{Init})	E_{50}^{ref} (kPa)	E_{oed}^{ref} (kPa)	E_{ur}^{ref} (kPa)	Power (m)	φ (degrees)	G_0^{ref}	$\gamma_{0.7}$	P_{ref} (kPa)	$k_{x,y}$ (m/day)
Model 1	1E-5	2.5	4,500	4,500	2E4	0.5	30	1E4	1E-4	30	8.6E-5
Model 2	1E-5	2.5	4,500	4,500	2E4	0.5	30	1E4	1E-4	30	0.15

Undrained analyses were performed with generation of pore pressures. The initial stresses were generated using a near-zero value of soil unit weight. Stresses were then generated in the ground by applying the 30kPa boundary stresses. Displacements were set to zero and the stone columns were expanded by applying a volume increase to achieve their as

built diameter. Each stone column cluster was set to dry as it was being expanded to simulate the drainage conditions. The mesh geometry after expansion of the stone columns is shown in Figure 9.

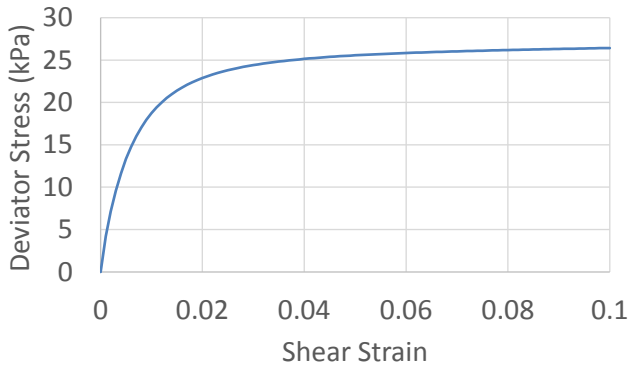

Figure 9: Results of triaxial simulation

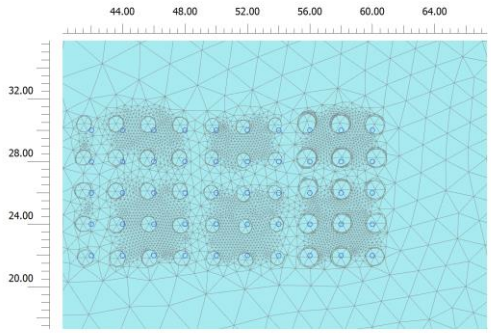

Figure 10: Mesh post stone column expansion

A comparison of lateral deformations at the location of the inclinometer with inclinometer measurements is shown in Figure 11 for Model 1 (In-situ permeability) and Model 2 (High permeability). Similar to cavity expansion theory, both models over predict lateral deformation with greatest lateral deformation being calculated using in-situ permeability. Excess pore pressures are compared in Figure 12 where it can be seen that both models under predict excess pore pressure. Model 1 using in-situ permeability was most similar to peak excess pore pressure during installation but Model 2 using a permeability about 2000 times higher was most similar to the rate of pore pressure dissipation.

The simulations suggest that the lateral displacements are affected by dissipation of pore pressures and that a much higher rate of pore pressure dissipation has occurred than the in-situ permeability would allow. A hypothesis to explain both smaller measured lateral deformations than calculated and higher rates of pore pressure dissipation is that installation of the stone columns causes the ground to fracture and temporarily heave until the fractures close. The theoretical volume strain would be partially dissipated by fracture heave and open fractures would enhance the rate of pore pressure dissipation. In Figure 12, the maximum excess pore pressure of 53kPa is approximately the same as the vertical effective stress at the depth of the piezometer. If the excess pore pressure exceeds the vertical effective stress at any depth then hydraulic fracture can occur. The data suggests that hydraulic fracture could have occurred within a radius of a few metres from each stone column as it was installed.

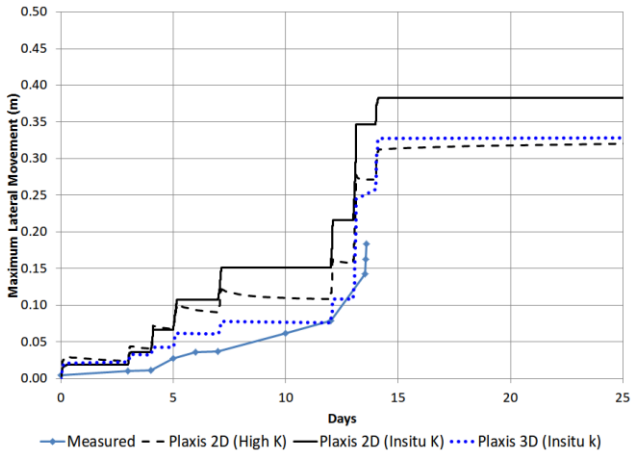

Figure 11: Lateral displacements

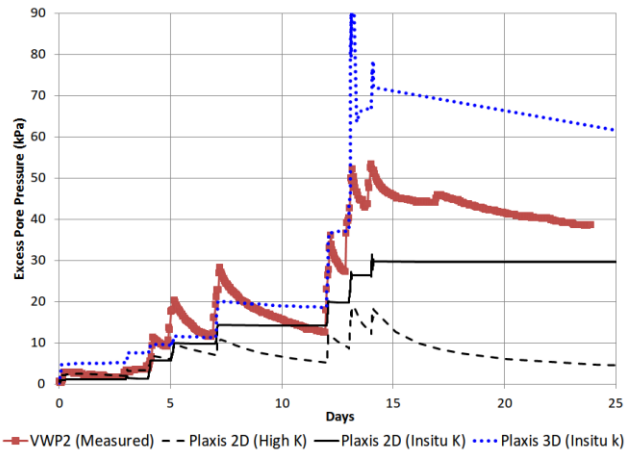

Figure 12: Excess pore pressures

5.2 PLAXIS 3D MODEL

The ground behaviour due to the installation of 50 individual stone columns was also examined using Plaxis 3D AE.02. The 3D finite element mesh adopted, measuring 45m long × 30m width × 12m depth, comprises an approximately 283,000 quadratic tetrahedral 10-node elements. Each of the 50 stone columns was modelled as an individual 12m long hexagonal prism, which has an equivalent cross section area to a circle of 300mm diameter. Hexagonal prisms were chosen to reduce the total number of 3D elements generated to within the computational limit.

The subsurface profile considered in the Plaxis 3D model comprises a 1m thick of gravel working platform constructed on site, underlain by 11m thick of soft clay with the properties as per Table 2. The groundwater level was modelled at the top of the soft clay. The soft clay was assumed to be normally consolidated during the initial stress generation. Prior to the installation of the stone columns, a 1m thick working platform was placed and the ground was allowed to consolidate to fully dissipate the excess pore pressure generated.

Installation of the individual stone columns was simulated in different consolidation calculation based on the actual construction sequence and installation timing. To simulate the expansion of stone columns during installation, the properties of the hexagonal prism, which initially modelled as an in-situ ground, was reassigned to stone column gravel and then simultaneously expanded radially through volumetric strains to form the final built diameter.

The deformed 3D mesh post stone columns expansion is shown in Figure 13. Comparisons of the lateral displacement and excess pore pressure prediction with measurements are shown Figures 11 and 12. Lateral displacements and excess pore pressures from the 3D modelling were closer to measurements than the 2D modelling, but lateral displacements were still over-predicted. The results of the 3D modelling show that large number of tension cut-off points were generated in the upper few metres of the soil profile (Figure 14), which suggested that fracturing of the ground occurs during stone column installation. The change in the ground permeability associated with fracturing, if any, is not captured in the finite element analysis.

Table 2: Material Properties used in Plaxis 3D analysis

Material	γ (kN/m^3)	E' (kPa)	φ' (degrees)	c'	$k_{x,y,z}$ (m/day)	Plaxis Material Drainage Type
Gravel working platform	21	30,000	45	0	0.6	Drained
Soft clay	16	4,500	30	0	8.6E-5	Undrained A
Stone column gravel	21	30,000	Elastic	Elastic	0.6	Drained

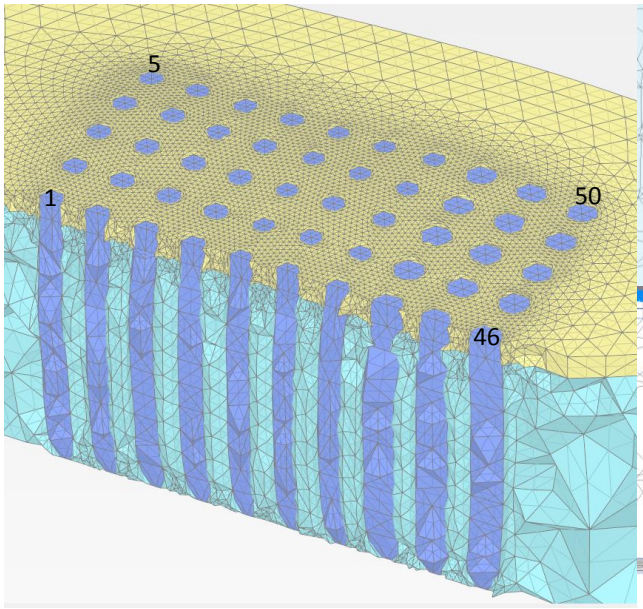

Figure 13: Deformed mesh post stone columns expansion

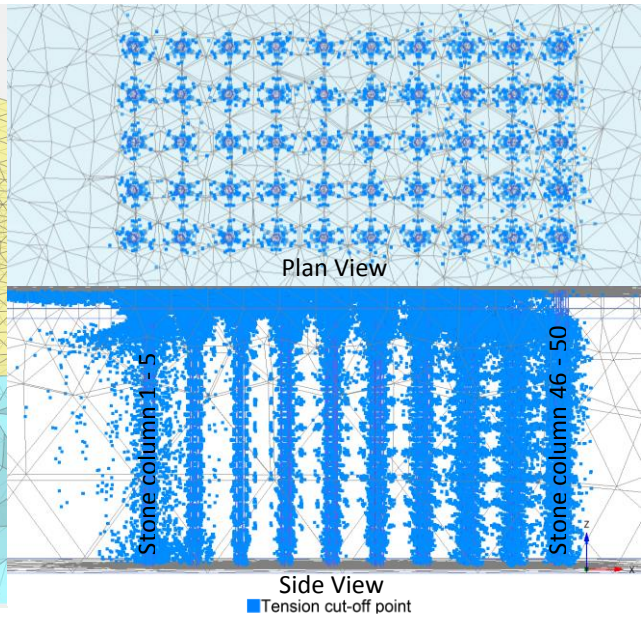

Figure 14: Tension point post stone column expansion

6 FINITE ELEMENT LIMIT ANALYSIS (FELA)

A second hypothesis for measured lateral displacements being less than predicted by analytical and numerical methods is that the clay may be forced between the stones and filling the voids within the stone column rather than expanding the cavity. An assessment of the pressure required for clay to flow pass stone particles has been performed using FELA. The stone particles are modelled as infinitely long cylinders within a rigid plastic medium. Pressures were calculated to push rigid plastic material past one, two, three and four rows of columns which are constructed at difference spacings in the horizontal and vertical directions. The geometry and failure mechanisms are shown in Figure 15.

Pressures required to develop failure mechanism in material with an undrained shear strength of 10kPa are plotted against the number of rows of cylinders for various horizontal centre to centre spacings (Sx) in Figure 16. The vertical spacing of the cylinders is held constant at 2D (D is the diameter of cylinders). Also shown in Figure 16 is a cavity expansion limit pressure calculated using Equation 4, where σ_{h0} is the initial horizontal stress (30kPa for consistency with the 2 dimensional finite element analyses). This assessment suggests that the limit pressure is capable of creating a plastic failure mechanism between one and four rows of cylinders depending on the spacing of the cylinders. Development of a plastic mechanism around an array of spheres is likely to require a higher pressure. By analogy, the data suggests that clay might only be forced a distance in the order of one to two stone particles into the stone columns as a result of lateral pressure created by cavity expansion as the particles will have a spacing of about 1D. Therefore it is considered unlikely that intrusion of clay into the stone columns causes the measured lateral displacement to be smaller than predicted by cavity expansion theory and finite element analysis.

$$P_{lim} = \sigma_{h0} + s_u \left(1 + \ln \frac{G_0}{s_u}\right) \quad (4)$$

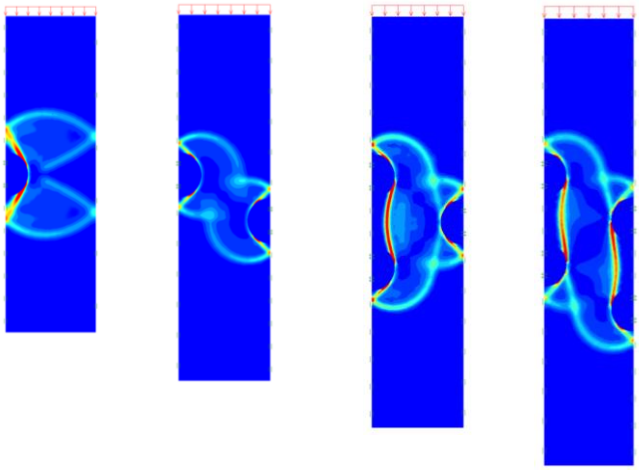

Figure 15: Geometry and FELA analyses

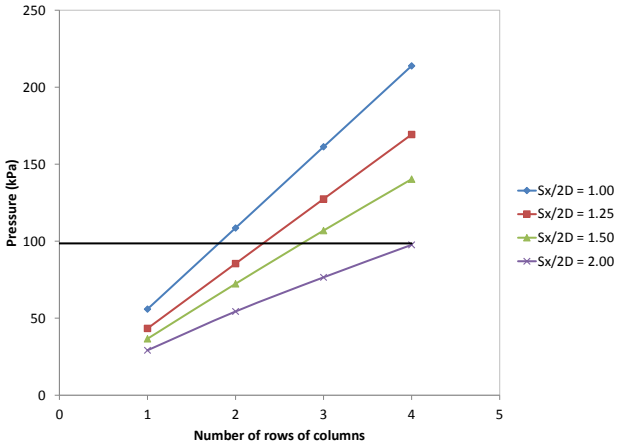

Figure 16 Pressure to create mechanism

7 CONCLUSIONS AND RECOMMENDATIONS

Measurements of lateral displacements and excess pore pressures during installation of a group of stone columns has been reported. These measurements have been compared with cavity expansion theory calibrated to measurements during installation of a single column and with 2D and 3D FEA. Cavity expansion and FEA calculations over predict lateral deformation and under predict excess pore pressure in general. The reason for this is postulated to be fracturing of the ground during stone column installation, and this hypothesis is supported by the excess pore pressure measurements and tension cut-off points generated during the 3D FEA.

The implication for design is that prediction of lateral soil deformation during stone column installation, and consequent effects on adjacent infrastructure, using numerical methods is potentially conservative. However, modelling fracturing of the ground is beyond the limit of current practice and a practitioner would need to use engineering judgement to develop empirical reduction factors to capture the effect on lateral deformation. It is the opinion of the authors that there is not sufficient data available in the literature to allow such an empirical correction to be made with confidence.

8 ACKNOWLEDGEMENTS

The Authors wishes to thank the Centre of Excellence for Geotechnical Science and Engineering for use of the data and Professor Andrei Lyamin (University of Newcastle) for the FELA analyses.

9 REFERENCES

Carter, J.P., Randolph, M.F. and Wroth, C.P. (1979) *Some aspects of the performance of open and closed ended piles*, Proc. Int. Conf. Num. Methods in Offshore Piling, ICE London, pp 165-170

Kelly, R.B., Muttuvel, T. and Chan, K.F. (2011) *Lateral displacements in soft soil due to installation of vibro-stone columns using the dry method*. Geofrontiers, Dallas, Texas, USA, pp. 549-546

Kelly, R.B., Pineda, J.A., Bates, L. & Suwal, L. (2016). *Site Characterisation for the Ballina Field Testing Facility* Geotechnique, submitted

Pineda, J.A., Suwal, L.P, Kelly, R.B., Bates, L and Sloan, S.W. (2016) *Characterisation of Ballina clay*, Géotechnique 66:7, 556-577
Yu, H-S (2000), *Cavity Expansion Methods in Geomechanics*, Kluwer Academic Publishers